Articles in PresS. Am J Physiol Regul Integr Comp Physiol (March 23, 2016). doi:10.1152/ajpregu.00541.2015

Calibrated variability of muscle sympathetic nerve activity during graded head-up tilt in humans and its link with noradrenaline data and cardiovascular rhythms

Andrea Marchi[1,2], Vlasta Bari[3], Beatrice De Maria[4],
Murray Esler[5], Elisabeth Lambert[5], Mathias Baumert[6], Alberto Porta[3,7]

[1] Department of Electronics Information and Bioengineering, Politecnico di Milano, Milan, Italy
[2] Department of Emergency and Intensive Care, San Gerardo Hospital, Monza, Italy
[3] Department of Biomedical Sciences for Health, University of Milan, Milan, Italy
[4] IRCCS Fondazione Salvatore Maugeri, Milan, Italy
[5] Human Neurotransmitter Laboratory, Baker IDI Heart and Diabetes Institute, Melbourne, Australia
[6] School of Electrical and Electronic Engineering, University of Adelaide, Adelaide, Australia
[7] Department of Cardiothoracic, Vascular Anesthesia and Intensive Care, IRCCS Policlinico San Donato, Milan, Italy

Running title: Spontaneous MSNA variability during orthostatic challenge

Address for correspondence:

Prof. Alberto Porta, PhD
Università degli Studi di Milano
Dipartimento di Scienze Biomediche per la Salute
IRCCS Policlinico San Donato
Laboratorio di Modellistica di Sistemi Complessi
Via F. Fellini 4
20097, San Donato Milanese
Milano, Italy

Tel: +39 02 52774382
Fax: +39 02 50319979
Email: alberto.porta@unimi.it

ABSTRACT

Muscle sympathetic nerve activity (MSNA) variability is traditionally computed through a low-pass filtering procedure requiring normalization. We proposed a new beat-to-beat MSNA variability preserving dimensionality typical of an integrated neural discharge (i.e. bursts per unit of time). The calibrated MSNA (cMSNA) variability is contrasted with the traditional uncalibrated MSNA (ucMSNA) version. The powers of cMSNA and ucMSNA variabilities in low frequency (LF, from 0.04 to 0.15 Hz) band were computed with those of heart period (HP), systolic and diastolic arterial pressure (SAP and DAP) in 7 healthy subjects (age: 20-28 years, median = 22 years, 5 females) during graded head-up tilt. Subjects were sequentially tilted at 0°, 20°, 30°, 40°, 60° table inclinations. The LF powers of ucMSNA and HP variabilities were expressed in normalized units (LFnu), while all remaining spectral markers were expressed in absolute units. We found that: i) the LF power of cMSNA variability was positively correlated with tilt angle, while the LFnu power of ucMSNA series was uncorrelated; ii) the LF power of cMSNA variability was correlated with LF powers of SAP and DAP, LFnu power of HP and noradrenaline concentration, while the relation of LFnu power of ucMSNA variability on LF powers of SAP and DAP was weaker and on LFnu power of HP was absent; iii) the stronger relation of cMSNA variability on SAP and DAP spectral markers compared to the ucMSNA series was confirmed individually. The cMSNA variability appears to be more suitable in describing sympathetic control in humans than traditional ucMSNA variability.

Keywords: Heart rate variability, arterial pressure variability, MSNA, catecholamines, autonomic nervous system, cardiovascular control.

INTRODUCTION

The spectral analysis of the spontaneous cardiovascular variability allows the indirect, noninvasive, inference of the autonomic function in humans (1, 20). The suitability of the spectral indexes derived from the beat-to-beat variations of heart period (HP), systolic and diastolic arterial pressure (SAP and DAP) has been validated by assessing their correlation with spectral indexes derived from direct, invasive, microneurographic recordings of muscle sympathetic nerve activity (MSNA) (5, 11, 28) during sympatho-inhibitory and/or sympatho-excitatory maneuvers (4, 10, 18, 21, 26). The link between MSNA and arterial pressure (AP) is widely recognized with MSNA burst rate increasing when AP falls and MSNA becoming silent when AP rises as a result of an operating baroreflex inhibiting sympathetic drive (29), even though central mechanisms such as the entrainment of a central oscillator by pulse-synchronous baroreceptor nerve activity cannot be excluded (2). Baroreflex-mediated modifications of the sympathetic drive are responsible for the changes of HP as well and partially explain the link between MSNA and HP variations (7). Traditionally the validation of the link between MSNA and modifications of HP and AP (mainly SAP and DAP in cardiovascular variability studies) was carried out after applying a suitable low-pass filtering procedure to the MSNA signal that retains the range of frequencies typical of cardiovascular variability (i.e. from 0 to 0.5 Hz) (4, 10, 18, 21, 26). Since the power of the MSNA signal in the low frequency (LF, from 0.04 to 0.15 Hz) band is significantly and positively correlated with the LF power of the HP variability, when expressed in normalized units, and with the LF power of SAP variability, when expressed in absolute units, it was suggested that HP and SAP spectral indexes, when expressed in suitable units, provide insight into autonomic regulatory mechanisms (21).

Since spectral indexes describing MSNA variability are traditionally computed directly from a low-pass filtered version of the MSNA signal (4, 10, 13, 18, 21, 26, 27, 31), these markers quantify the magnitude of changes in burst amplitude and area about their mean value more than the variations in their rate of occurrence. In other words, the variability series of MSNA, as currently derived from the MSNA signal, has the same physical dimension of the MSNA signal (i.e. mV) and does not have the physical dimension of a neural discharge (i.e. bursts per unit of time). As a consequence, the spectral indexes derived from MSNA variability depend on numerous factors including the number of active fibers, the proximity to the recording electrode to the bundle, the operator experience to pick up the nerve, the setting of the acquisition system (e.g. the gain of the neural traffic amplifier) and the level of the noise superimposed to the MSNA signal. These factors increase the within- and between-subject variability and their influence is usually mitigated by normalization procedures taking the form of the division by the variance of the MSNA variability in

baseline condition (27) or by the variance minus the power in the very low frequency (VLF) band (i.e. below 0.04 Hz) (21).

We hypothesize that the traditional low-pass filtered MSNA variability signal has limited power in tracking the magnitude of the response of the cardiovascular control to a sympatho-excitatory stimulus, is intrinsically exposed to influences of noise and blurs physiological relations with more traditional cardiovascular variabilities that, conversely, might be highlighted by exploiting a different definition of MSNA variability.

In this study we propose a new approach for obtaining a beat-to-beat MSNA variability from the integrated MSNA signal, referred to as calibrated MSNA (cMSNA) variability. In contrast to the one currently in use, referred to as uncalibrated MSNA (ucMSNA) variability, it has the desirable characteristic of assessing directly the modulations of the burst frequency, thus exhibiting the dimensionality of a neural discharge signal (i.e. number of bursts per unit of time). The LF power derived from the cMSNA variability was computed during a graded head-up tilt protocol inducing a sympathetic activation and vagal withdrawal according to the inclination of the tilt table in healthy volunteers (3, 4, 9, 10, 13, 14, 16, 17, 23). In this study we evaluated the relation of the LF power of cMSNA variability with: i) the tilt table angles; ii) plasma noradrenaline (NA) concentration and spillover; iii) traditional indirect noninvasive spectral indexes derived from HP, SAP and DAP series; iv) the LF power of the ucMSNA variability.

MATERIALS AND METHODS

Experimental Protocol and Data Acquisition

The study comprised 7 healthy subjects (age from 20 to 28 years, median = 22 years; BMI: from 21 to 29 kg/m^2, median = 24 kg/m^2; 5 females). The study protocol was approved by the Alfred Hospital Ethics Review Committee (n. 144/06) and conformed to the relevant guidelines of the National Health and Medical Research Council of Australia and to the principles of the Declaration of Helsinki for medical research involving humans. All subjects provided written informed consent. The head-up tilt protocol was fully described in (14). Briefly, all subjects were tested in the morning, after a light breakfast. Caffeine and alcohol intake was excluded from 7:00 PM on the evening before the study. The radial artery was cannulated percutaneously (3F, 5 cm, Cook catheter) to enable AP monitoring and blood sampling for catecholamine measurement. A lead III ECG was recorded. Respiration movements were monitored via piezoelectric device (ADI Instruments, Australia). Multiunit sympathetic nerve firing rates in postganglionic fibers distributed to the skeletal muscle vasculature were recorded by using clinical microneurography as previously described (14). After locating the common peroneal nerve, a tungsten microelectrode (FHC,

Bowdoinham, Maine) was inserted percutaneously and adjusted until satisfactory spontaneous MSNA was observed in accordance with previously described criteria (14). After instrumentation, subjects were allowed to rest for at least 30 minutes. Then, subjects were sequentially tilted to 0°, 20°, 30°, 40° and 60° (T0, T20, T30 T40 and T60 respectively) for 10 minutes at each angle. The head-up tilt test started from the horizontal position and was incremental with respect to the previous tilt table inclination, thus allowing us to maintain the positioning of the microelectrodes in the same subject and to preserve an invariable quality of the MSNA recordings over the entire experimental session. AP, ECG, respiratory rate, and MSNA were measured at each tilt angle. The raw MSNA signal was band-pass filtered (700 – 2000 Hz), amplified, rectified, and integrated (time constant of 0.1 s) to obtain integrated MSNA. AP, ECG, respiratory movements and integrated MSNA, were digitized at 1000 Hz using PowerLab (model ML785/8SP, ADI Instruments, Australia) and recordings were stored for off-line analysis. Blood samples were taken at the end of each head-up tilt session including T0, and all other parameters were collected continuously. The plasma NA concentration and the NA appearance rate (i.e. spillover) was determined as previously described in (14). No subject exhibited presyncope signs during the orthostatic challenge.

Extraction of the Beat-to-Beat HP and AP Variability Series

The R-wave peaks on the ECG were located with minimum jitters using parabolic interpolation. The temporal distance between two consecutive parabolic apexes was taken as HP approximation. The maximum of AP inside the i-th HP was defined as the i-th SAP value, where i is the cardiac beat counter. The i-th DAP was computed as the minimum of AP following the i-th SAP. The respiratory signal provided an estimate of the respiratory rate. The occurrences of R-wave peaks, SAP and DAP fiducial points were carefully checked to avoid erroneous detections or missed beats. The beat-to-beat series of HP = {HP(i), i = 1,..., N}, SAP = {SAP(i), i = 1,..., N} and DAP = {DAP(i), i = 1,..., N} were extracted, where N is the series length. Sequences with N = 256 consecutive measures were selected at random in each experimental session. The series were linearly detrended. If nonstationarities, such as very slow drifting of the mean or sudden changes of the variance, were evident despite the linear detrending, the random selection was carried out again. The mean and the variance of HP, SAP and DAP were indicated as μ_{HP}, σ^2_{HP}, μ_{SAP}, σ^2_{SAP}, μ_{DAP} and σ^2_{DAP}, and expressed as ms, ms^2, mmHg, mmHg^2, mmHg and mmHg^2 respectively. From the MSNA signal we computed the burst frequency and incidence, indicated as bf_{MSNA} and bi_{MSNA}, and expressed as bursts/minute and bursts/100 beats respectively.

MSNA Beat-to-Beat Series Extraction

The *i*-th ucMSNA value was obtained by dividing the integral computed over the integrated MSNA signal between the (*i*-1)-th and *i*-th DAP values by the inter-diastolic interval (21). The extraction of the cMSNA variability requires the detection of the MSNA bursts from the integrated MSNA signal. Sympathetic bursts were detected by an adaptive thresholding where the burst detection threshold was updated on a beat-to-beat basis to follow baseline wandering and physiological variations of the MSNA burst amplitude (6). The MSNA peaks overcoming the adaptive threshold were considered as MSNA bursts. To account for the latency from the AP sensing to the possible sympathetic response (12, 32), the MSNA burst was searched in a temporal window ranging from 0.9 to 1.7 s starting from the R-wave peak of the first R-wave peak delimiting the current HP (6). The cMSNA signal was obtained from the integrated MSNA signal (Fig.1c) by counting the number of MSNA bursts inside a moving time window of 5 s, thus obtaining a step-wise count MSNA signal (Fig.1d), and by low-pass filtering the step-wise count MSNA signal (Fig.1e) with a finite impulse response filter with a cut-off frequency of 0.5 Hz (8000 coefficients), thus retaining exclusively the frequency range of cardiovascular variability. As expected from the physiological relation between MSNA and AP (29), the step-wise count MSNA (Fig.1d) and its filtered version (Fig.1e) are in phase opposition with the LF oscillations of AP, clearly visible as the modulation of SAP and DAP values over time (Fig.1b). Finally, the low-pass count MSNA signal was down-sampled once per cardiac beat at the occurrence of the first R-wave peak delimiting the *i*-th HP as detected from the ECG (Fig.1a). The resulting time series was expressed in burst/s by dividing the count cMSNA values by the length of the time window. As a consequence of these definitions the beat-to-beat variability of both cMSNA = {cMSNA(*i*), *i* = 1,..., *N*} and ucMSNA = {ucMSNA(*i*), *i* = 1,..., *N*} were synchronous with the beat-to-beat variability series of HP, SAP and DAP.

Autoregressive Power Spectral Analysis

The power spectrum was estimated according to a univariate parametric approach fitting the series with an autoregressive model (20). Autoregressive spectral density was factorized into components, each of them characterized by a central frequency. A spectral component was labeled as LF if its central frequency lay in LF band, while it was classified as high frequency (HF) if its central frequency was between 0.15 and 0.5 Hz (30). The LF and HF powers were defined as the sum of the powers of all LF and HF spectral components, respectively.

The following spectral indexes were computed: 1) the LF power of HP series expressed in normalized units ($LFnu_{HP}$), defined as the LF power of the HP series multiplied by 100 and divided by the σ^2_{HP} minus the power of HP series in the VLF band, deemed to be an index of sympathetic

modulation directed to the heart (20); 2) the HF power of HP series (HF_{HP}) expressed in absolute units (i.e. ms^2) considered to be a marker of vagal modulation directed to the heart (1); 3) the LF_{HP}/HF_{HP} ratio, a dimensionless index obtained by dividing the LF power by the HF one both computed over the HP series, deemed to be an indicator of the sympatho-vagal balance to the heart (20); 4) the LF powers of SAP and DAP (LF_{SAP} and LF_{DAP}), expressed in absolute units (i.e. $mmHg^2$), considered to be indexes of sympathetic modulation directed to the vessels. The LF power of cMSNA series (LF_{cMSNA}) expressed in absolute units (i.e. $bursts^2/s^2$) was taken as a direct invasive index of sympathetic modulation. The LF power of ucMSNA series expressed in normalized units ($LFnu_{ucMSNA}$), defined as the LF power of the ucMSNA variability multiplied by 100 and divided by the σ^2_{ucMSNA} minus the power of the ucMSNA variability in the VLF band, was computed as a direct invasive index of sympathetic modulation (21). The normalization procedure applied to the LF power of the ucMSNA variability was necessary because the ucMSNA series had the same dimension of the MSNA signal (i.e. mV) and the amplitude of its oscillations was arbitrary and depended on factors largely independent of the burst rate.

Statistical Analysis

We carried out the Bartlett test, or the Levene test when appropriate, to check for homoscedasticity of the computed parameters in the various experimental sessions. If the test did not pass we carried out a log-transformation and the test for the homogeneity of variance was repeated. One way repeated measures analysis of variance, or Friedman repeated measures analysis of variance on ranks when appropriate, (Student-Newman-Keuls's test for multiple comparisons) was applied to test the significant changes of time, frequency domain and NA data compared to T0. Linear regression analysis was carried out to check the association of LF_{SAP}, LF_{DAP}, $LFnu_{HP}$, HF_{HP}, LF_{cMSNA} and $LFnu_{ucMSNA}$ indexes on tilt table angles. The Pearson product-moment correlation coefficient, *r*, was computed and the null hypothesis of a slope equal to 0 (i.e. no linear relationship) was tested. The same analysis was carried out to assess the correlations of spectral indexes derived from cMSNA or ucMSNA variability (i.e. LF_{cMSNA} and $LFnu_{ucMSNA}$ powers) with NA data and traditional frequency domain indexes derived from SAP, DAP and HP series (i.e. LF_{SAP}, LF_{DAP}, $LFnu_{HP}$, HF_{HP}). *r* was calculated after pooling together the values derived from all subjects regardless of the experimental condition. Additionally, squared *r*, r^2, was computed for each subject to assess individually the degree of association of traditional spectral indexes on LF_{cMSNA} or $LFnu_{ucMSNA}$ powers. Individual correlation analyses were carried out only if the correlation analysis performed after pooling all subjects together was significant over both cMSNA and ucMSNA series. An individual $r^2 > 0.5$ was taken as significant and the fraction of subjects with $r^2 > 0.5$ was

computed. Statistical analysis was carried out using a commercial statistical program (Sigmaplot, Systat Software, Inc, Chicago, IL, USA, ver.11.0). Values were reported as mean ± standard deviation. A $p < 0.05$ was always considered statistically significant.

RESULTS

Figure 2 shows an example of ucMSNA (Figs.2a,b) and cMSNA (Figs.2e,f) variability derived from the same subject during T0 (Figs.2a,e) and T60 (Figs.2b,f) and the corresponding autoregressive power spectral density (Figs.2c,d and Figs.2g,h, respectively). The magnitude of the oscillations of both ucMSNA and cMSNA variabilities increased evidently during T60 compared to T0. The power spectral density of both ucMSNA and cMSNA variabilities exhibited a dominant peak in the LF band that became sharper during T60 compared to T0. The cMSNA variability is less noisy at higher frequencies (i.e. close to 0.5 Hz) than the ucMSNA series.

Results of time domain analyses of HP, SAP, DAP series and MSNA signals as well as NA concentration and spillover values were summarized in Table 1. With the increase of the intensity of the orthostatic stimulus the μ_{HP} significantly decreased as early as during T20 compared to T0 and progressively declined with tilt table inclination. Conversely, μ_{SAP} remained stable and μ_{DAP} increased solely during T60. We found that the σ^2_{HP} was highly sensitive to the orthostatic challenge, being decreased during T20, T40 and T60. Conversely, both the σ^2_{SAP} and σ^2_{DAP} increased solely at the highest tilt table inclination (i.e. during T60). While the tonic sympathetic activity, expressed as bf_{MSNA}, increased as early as during T30 and remained higher during T40 and T60, the bi_{MSNA} was unaffected by the orthostatic challenge. While NA concentration increased during T40 and T60, NA spillover remained stable.

Results of frequency domain analyses are given in Table 2. The $LFnu_{HP}$ power significantly increased during T40 and T60 compared to T0, while the LF_{HP}/HF_{HP} ratio augmented solely during T60. Conversely, the HF_{HP} power significantly decreased as early as during T20 and progressively declined with tilt table angle. The LF_{SAP} and LF_{DAP} powers rose significantly only at the highest tilt table angle (i.e. during T60). The LF_{cMSNA} power increased significantly during T40 with respect to T0, while the $LFnu_{ucMSNA}$ index was unaffected by the orthostatic challenge.

Figure 3 shows the individual values (open circles) of the LF_{cMSNA} (Fig.3a) and $LFnu_{ucMSNA}$ (Fig.3b) powers as a function of the tilt table inclination. A significant positive association of the LF_{cMSNA} power with tilt table angle (r=0.377, p=$2.79 \cdot 10^{-2}$) was found. On the contrary, the $LFnu_{ucMSNA}$ power was uncorrelated with tilt table inclination.

Figure 4 shows the individual values (open circles) of the LF_{SAP} (Fig.4a), LF_{DAP} (Fig.4b), $LFnu_{HP}$ (Fig.4c) and HF_{HP} (Fig.4d) powers as a function of the tilt table inclination. All indirect,

noninvasive, spectral indexes were significantly correlated with tilt table inclination but, while the LF_{SAP}, LF_{DAP} and $LFnu_{HP}$ powers were positively related with the intensity of the orthostatic stimulus (r=0.43, p=1.11·10^{-2}, r=0.434, p=1.03·10^{-2} and r=0.486, p=3.59·10^{-3} respectively), the HF_{HP} marker was negatively correlated (r=-0.769, p=1.08·10^{-7}).

Figure 5 shows the results of the linear correlation analysis between the $LFnu_{ucMSNA}$ power and spectral indexes derived from HP, SAP and DAP series. The degree of association was computed after pooling all subjects together regardless of the experimental condition. We found that the $LFnu_{ucMSNA}$ marker exhibited a positive correlation with the LF_{SAP} (Fig.5a) and LF_{DAP} (Fig.5b) indexes (r=0.428, p=1.16·10^{-2} and r=0.402, p=1.86·10^{-2} respectively), but it was uncorrelated with the $LFnu_{HP}$ (Fig.5c) and HF_{HP} (Fig.5d) powers.

Figure 6 shows the results of linear correlation analysis between the LF_{cMSNA} power and spectral indexes derived from HP, SAP and DAP series. The degree of association was computed after pooling all subjects together regardless of the experimental condition. The correlation between the LF_{cMSNA} marker and LF_{SAP} index (Fig.6a) was positive and significant (r=0.69, p=6.28·10^{-6}). The same result held when the LF_{DAP} power (Fig.6b: r=0.74, p=5.75·10^{-7}). The LF_{cMSNA} power was positively correlated with the $LFnu_{HP}$ marker (Fig.6c, r=0.417, p=1.4·10^{-2}) as well. Conversely, it was uncorrelated with HF_{HP} power (Fig.6d).

Table 3 shows the results of correlation analysis of catecholamine data (i.e. NA concentration and spillover) on spectral variability indexes. Pearson product-moment correlation coefficient, r, and type I error probability, p, was reported. NA concentration was uncorrelated with $LFnu_{HP}$ and LF_{HP}/HF_{HP} indexes, it was positively correlated with LF_{SAP}, LF_{DAP}, $LFnu_{unMSNA}$ and LF_{cMSNA} powers and negatively correlated with the HF_{HP} marker. NA spillover was unrelated with all spectral variability indexes.

In Table 4 we reported the fraction of subjects featuring a squared correlation coefficient, r^2, larger than 0.5 between traditional spectral indexes and MSNA markers computed in the LF band over cMSNA (i.e. LF_{cMSNA}) and ucMSNA (i.e. $LFnu_{ucMSNA}$) variabilities. Correlation analysis was carried out on a case-by-case basis provided that the association between the same variables computed after pooling all subjects together was significant over both cMSNA and ucMSNA series. This situation occurred solely when the LF_{SAP} or LF_{DAP} markers were considered: indeed, the HF_{HP} power was uncorrelated with either the $LFnu_{ucMSNA}$ or LF_{cMSNA} index and the $LFnu_{HP}$ power was significantly correlated with the LF_{cMSNA} marker but uncorrelated with the $LFnu_{ucMSNA}$ power, thus suggesting that the relation of the $LFnu_{HP}$ to LF_{cMSNA} index was tighter than that to the $LFnu_{ucMSNA}$ power. The fraction of subjects with r^2 larger than 0.5 between the LF_{SAP} power and $LFnu_{ucMSNA}$ marker was lower than that between the LF_{SAP} power and LF_{cMSNA} index (i.e. 2 versus 5 out of 7

respectively). Similar fractions were found between the LF_{DAP} power and $LFnu_{ucMSNA}$ marker and between the LF_{DAP} power and LF_{cMSNA} index (i.e. 1 versus 5 out of 7 respectively). This finding indicates a better suitability of the cMSNA variability in describing the LF oscillations of sympathetic activity responsible for slow SAP and DAP fluctuations compared to the ucMSNA series.

DISCUSSION

The findings of the present study can be summarized as follows: i) we propose a new procedure to derive a MSNA variability (i.e. the cMSNA series) preserving the dimensionality of a neural discharge signal by assessing directly the modulation of the burst frequency; ii) the LF power of the cMSNA series is positively related to the tilt table angle, while the normalized LF power of ucMSNA series is unrelated to it; iii) the LF power of the cMSNA variability is positively associated with the LF powers of SAP and DAP series and with the normalized LF power of HP series; iv) the association of the normalized LF power of the ucMSNA variability with the power of SAP and DAP series is weaker and even absent with the normalized LF power of HP series; v) the LF power of the cMSNA variability and the normalized LF power of the ucMSNA series are unrelated to the HF power of HP series; vi) the LF power of the cMSNA variability and the normalized LF power of the ucMSNA series are correlated with NA concentration; vii) individual regression lines confirm a stronger link of the cMSNA index in the LF band to the SAP and DAP spectral markers compared to that computed over the ucMSNA variability as a likely result of the better suitability of the cMSNA series in describing the variability of the sympathetic discharge.

The cMSNA Variability is more Suitable than its ucMSNA Version in Describing Sympathetic Control

This study proposes a new procedure for the extraction of the MSNA variability (i.e. the cMSNA series), validates it using a graded head-up tilt protocol and correlates spectral indexes extracted from it with those derived from traditional HP, SAP and DAP variability series. The LF power of the cMSNA variability increased gradually with the tilt table inclination. This finding suggests that the amplitude of the variations of the neural discharge about its mean value rises with the magnitude of the orthostatic stimulus and stresses that, in addition to a tonic increase of the mean sympathetic activity, here confirmed by the increase of NA concentration, also the modulation of the sympathetic discharge increases with the magnitude of the orthostatic stressor. This finding is not surprising given that the correlation between the MSNA variability and tilt table angles is well-known using a more traditional definition of MSNA variability but here it is detected

as early as during T40 (4, 10, 13). This finding is in agreement with those linking the MSNA variability in the LF band to the intensity of the sympathetic activation induced by graded lower body negative pressure protocol (26) or by modifications of AP values (21, 27).

At difference with the traditional definition of MSNA variability, the cMSNA series allows us to preserve the dimensionality of the neural discharge signal (i.e. bursts per second) because the cMSNA variability is directly related to the modulation of the burst frequency. As a consequence of its physical dimensionality it does not require normalization procedures helpful to compare different subjects. Conversely, normalization procedures are mandatory in case of the traditional low-pass filtered MSNA variability because factors that have nothing to do with neural traffic but that can alter the amplitude and area of the MSNA bursts, such as the position of the electrode, its proximity to the bundle, number of active units, amplification gain, and effects of noise superposed to the MSNA signal, might profoundly influence conclusions. The reduction of the impact of these factors is responsible for the less noisy nature of the cMSNA variability compared to the traditional low-pass filtered MSNA variability and contributes to keep under control the within- and between-subject variability, thus improving the statistical power of the analysis. As a result the LF power of the cMSNA variability was significantly related to tilt table inclination, while the LF power of the ucMSNA series was unrelated to it, and the association of the LF power of cMSNA series with traditional noninvasive spectral indexes of sympathetic modulation was stronger than that found using the ucMSNA variability regardless of whether the analysis was carried out after pooling all subjects together or on a case-by-case basis.

Traditional Cardiovascular Variability Indexes in Time and Frequency Domains during Graded Head-up Tilt

Head-up tilt is one of the most utilized maneuvers to induce a sympathetic activation and vagal withdrawal mainly driven by a reduction of venous return and central blood volume and consequent baroreflex unloading (4, 19, 24). Here we confirm the traditional findings relevant to time and frequency domain analyses of HP, SAP and DAP series (3, 4, 9, 10, 13, 14, 16, 17, 23, 26). More specifically, the HP mean decreased significantly and the HP variance declined as well. Conversely, as expected the SAP mean did not vary, while the SAP variance, DAP mean and DAP variance significantly increased at the highest tilt table inclination (i.e. during T60). Spectral indexes exhibited the expected trends with tilt table angles as well. More specifically, the LF powers of SAP and DAP series, the normalized LF power of HP variability and the ratio of the LF to the HF power computed over HP series increased and the HF power of HP variability steadily decreased.

cMSNA and ucMSNA Variability Indexes in Time and Frequency Domains during Graded Head-up Tilt

Time domain indexes derived from the MSNA signal indicated that our head-up tilt protocol elicited the expected tonic sympathetic activation (3, 4, 9, 10, 13, 14, 26). Indeed, burst frequency significantly increased, and the same trend was observed in the case of the burst incidence even though the increase did not reach statistical significance. This finding was also confirmed by the rise of the NA concentration at tilt table angles larger than or equal to 40°.

The LF power of the cMSNA variability gradually increased with tilt table, thus suggesting that head-up tilt increases the amplitude of the changes of the sympathetic discharge (i.e. the variation of the sympathetic tonic activity about its mean value). Since this modification occurred in the LF band, this finding is likely to be unrelated to respiratory modulation of MSNA signal and more likely to be related to slower AP regulatory mechanisms (4, 10, 13, 18, 21, 26, 27). Contrary to the expectations, the normalized LF power of the ucMSNA variability was unrelated to tilt table angles. Since a significant relation with tilt table angle is expected (4, 10, 13, 21, 26), this lack indicates that the normalized LF power of the ucMSNA variability cannot deal with the smallness of the sample size and the low intensity of the orthostatic stimulus (i.e. subjects did not undergo orthostatic challenges with tilt table inclinations steeper than 60 degrees). Conversely, the significant correlation of the LF power of cMSNA series with tilt table angles indicates that this index is more powerful in tracking the modifications of the sympathetic control during graded head-up tilt, especially when sample size is small and the intensity of the stimulus is limited (i.e. at small tilt table angles). It is worth noting that both indexes (i.e. the LF power of cMSNA variability and the normalized power of ucMSNA series) were correlated with NA concentration and unrelated to NA spillover.

Comparing the Relations of cMSNA and ucMSNA Spectral Indexes to Indirect, Noninvasive, Autonomic Markers derived from HP, SAP and DAP Series

The LF power of SAP and DAP series was proposed as an indirect, noninvasive, marker of the sympathetic modulation directed to the vessels because it was significantly associated to the LF power of the ucMSNA variability (21). Ryan et al. (26) confirmed the strong correlation between the LF power of SAP series and the LF power of the ucMSNA series during the sympathetic activation induced by graded lower body negative pressure test. However, Ryan et al. (26) found that, when the analysis was carried out individually, this relation disappeared, thus indicating a poor within-subject reproducibility during both the same recording session and across days. As a consequence, Ryan et al. (26) concluded that the amplitude of the LF oscillations of SAP and DAP

could not be used as non-invasive surrogates of direct, invasive, measure of modulation of sympathetic activity as derived from the MSNA variability. This conclusion might be the consequence of the use of an ucMSNA series and to the lack of the application of any normalization procedure to the MSNA parameters being both factors increasing the within-subject variability. These factors might be responsible for the disagreement observed between the LF marker derived from the ucMSNA variability and the LF power of SAP and DAP variabilities reported by Taylor et al. (31) as well.

One of the major findings of this study is that the associations of the LF power of cMSNA variability with the spectral indexes in the LF band derived from HP, SAP and DAP series are much stronger than those computed when the normalized LF power of ucMSNA variability was considered. The association of the LF power of cMSNA variability with the spectral markers in the LF band derived from SAP and DAP series was found in a larger fraction of subjects compared to the association of the normalized LF power of ucMSNA variability and the same spectral indexes. We suggest that at least part of the disagreement observed in Ryan et al. (26) and in Taylor et al. (31) might be attributable to the factors independent of the physiology of the cardiovascular control and affecting importantly any traditional definition of the ucMSNA variability based on low-pass filtering procedure. We hypothesize that, if the ucMSNA variability was substituted with the cMSNA series, conclusions might be different. In addition, we remark that the LF power of cMSNA expressed in absolute units remained unrelated to the HF power of the HP series, thus stressing the independence of this index from vagal modulation.

Interpretation of the Correlation between cMSNA Spectral Parameters and Indirect, Noninvasive, Autonomic Markers derived from HP, SAP and DAP Series

The global correlation of the LF power of cMSNA variability with LF indexes of SAP and DAP series, confirmed even individually in the majority of subjects, suggests that the LF power of SAP and DAP series can be utilized as a noninvasive marker of the sympathetic modulation directed to vessels (21). This conclusion was supported by the correlation of NA concentration with SAP and DAP spectral indexes. The correlation of the LF power of cMSNA variability with the normalized LF power of HP series supports the utilization of this index as a marker of sympathetic modulation directed to the heart (21). Since the LF power, when expressed in absolute units, is under sympathetic and vagal controls (22) and the proportion of these influences is unknown, this result might be surprising, especially because in our experimental protocol the magnitude of the orthostatic challenge is limited and, as a consequence, vagal modulation in the LF band might be preponderant over the sympathetic contribution. The normalization of the LF power might be

436 responsible for the observed significant link with the LF power of cMSNA variability. However,
437 one factor deserves attention. The absence of a correlation between the LF power of cMSNA series
438 and the HF power of HP series challenges the existence of a sympatho-vagal balance in the form
439 that the rise of the sympathetic control implies, by necessity, a withdrawal of the vagal regulation
440 and *vice versa* (15). Indeed, if the concept of sympatho-vagal balance held in our experimental
441 protocol, the two indexes should be negatively correlated. Since the normalized LF power of the HP
442 series, in conjunction with the normalized HP power of HP series, was designed to quantify the
443 concept of sympatho-vagal balance because when the normalized LF power raises, the normalized
444 HF power declines and *vice versa* (15, 20) given that their sum is 100 (8, 23), the correlation of the
445 normalized LF power of HP series with the LF power of cMSNA variability could misrepresent the
446 underlying physiology because it leads necessarily to a correlation of LF power of cMSNA
447 variability with the normalized HF power of HP series. This same reasoning applies to the ratio of
448 the LF to the HF power computed over HP series. This conclusion is supported by the lack of
449 correlation of NA concentration on both normalized LF power and ratio of the LF to the HF power
450 computed over HP series.
451
452 *Limitations of the Study and Future Developments*
453 Correlations, even though statistically significant according to the adopted level of significance,
454 are weak in absolute terms. We advocate future studies to test the results on a larger database,
455 maybe created ad-hoc through a joint project associating several laboratories in different countries
456 to get the optimal sample size, and to check whether increasing the number of subjects could lead to
457 the expected improvement of the squared correlation coefficient. Also the extension of the range of
458 intensity of the orthostatic stimulus might be helpful to test whether the observed rise of the LF
459 power of cMSNA variability with the tilt table inclination continues or a saturation occurs.
460 In addition to the limited size of the sample, this study might suffer for the peculiarity of using
461 an incremental head-up tilt test that did not randomize the challenge (i.e. the tilt table inclination)
462 and did not allow the subject to return in the horizontal position. This choice was very helpful
463 because it minimized the likelihood of losing the positioning of the microelectrodes during MSNA
464 recordings but it has the drawback of introducing a time dependency in the measures that is not
465 directly tackled by our statistical analysis. Future studies should test the possibility of monitoring
466 the cMSNA variability with an adequate sample size in protocols randomizing the challenge and
467 allowing the return in the horizontal position.
468
469 *Perspectives and Significance*

The study employed a new approach to obtain a cMSNA variability preserving the dimensionality of a neural discharge (i.e. bursts per second). The defined cMSNA variability limits the effect of factors that directly affect the quality of the MSNA recordings by altering amplitude and area of the bursts. The validation, carried out over a protocol inducing a progressive sympatho-excitation, suggests that the LF power of the cMSNA series can track the increase of the sympathetic modulation associated to the increased intensity of the orthostatic stimulus. The important association of the spectral indexes derived from cMSNA series with those derived from spontaneous fluctuations of cardiovascular variables in the LF band noninvasively derived from ECG and AP recordings, found both globally (i.e. over the entire population) and individually in a significant fraction of subjects, stresses the usefulness of indirect, noninvasive, spectral indexes in assessing autonomic function. In addition, it suggests that part of the disagreement observed between traditional MSNA variability indexes and HP, SAP and DAP spectral markers in the LF band might be due to the intrinsic weakness of the ucMSNA variability more than to the physiology of the cardiovascular control. Therefore, this study prompts for the exploitation of the cMSNA series, instead of the more traditional ucMSNA, in studies modeling cardiovascular variability interactions (25) and integrating direct measures of sympathetic activity in suitable descriptions of the cardiovascular control (9).

GRANTS

This study was supported by the Australian Research Council (DP110102049).

DISCLOSURES

No conflicts of interest, financial or otherwise, are declared by the authors,

AUTHOR CONTRIBUTIONS

A.P. conception and design of research; M.E. and E.L. performed experiments; A.M. analyzed data; A.M. V.B., B.D.M., M.E., E.L. M.B., and A.P. interpreted results of experiments; A.M. prepared figures; A.M. and A.P. drafted manuscript; A.M. V.B., B.D.M., M.E., E.L. M.B., and A.P. edited and revised manuscript; A.M. V.B., B.D.M., M.E., E.L. M.B., and A.P. approved final version of manuscript.

References

1. **Akselrod S, Gordon D, Ubel FA, Shannon DC, Berger AC, Cohen RJ.** Power spectrum analysis of heart rate fluctuation: a quantitative probe of beat-to-beat cardiovascular control. *Science* 213: 220-222, 1981.
2. **Barman SM, Fadel PJ, Vongpatanasin W, Victor RG, Gebber GL.** Basis for the cardiac-related rhythm in muscle sympathetic nerve activity of humans. *Am J Physiol* 284: H584–H597, 2003.
3. **Baumert M, Lambert E, Vaddadi G, Sari CI, Esler M, Lambert G, Sanders P, Nalivaiko E.** Cardiac repolarization variability in patients with postural tachycardia syndrome during graded head-up tilt. *Clin Neurophysiol* 122: 405-409, 2011.
4. **Cooke WH, Hoag JB, Crossman AA, Kuusela TA, Tahvanainen KU, Eckberg DL.** Human responses to upright tilt: a window on central autonomic integration. *J Physiol* 517: 617-628, 1999.
5. **Delius W, Hagbarth KE, Hongell A, Wallin BG.** General characteristics of sympathetic activity in human muscle nerves. *Acta Physiol Scand* 84: 65-81, 1972.
6. **Diedrich A, Porta A, Barbic F, Brychta RJ, Bonizzi P, Diedrich L, Cerutti S, Robertson D, Furlan R** Lateralization of expression of neural sympathetic activity to the vessels and effects of carotid baroreceptor stimulation. *Am J Physiol* 296: H1758-H1765, 2009.
7. **Eckberg DL.** Temporal response patterns of the human sinus node to brief carotid baroreceptor stimuli. *J Physiol* 258: 769-782. 1976.
8. **Eckberg DL.** Sympathovagal balance: a critical appraisal. *Circulation* 96: 3224-3232, 1997.
9. **El-Hamad F, Lambert EA, Abbott D, Baumert M.** Relation between QT interval variability and muscle sympathetic nerve activity in normal subjects. *Am J Physiol* 309: H1218-H1224, 2015.
10. **Furlan R, Porta A, Costa F, Tank J, Baker L, Schiavi R, Robertson D, Malliani, Mosqueda-Garcia R.** Oscillatory patterns in sympathetic neural discharge and cardiovascular variables during orthostatic stimulus. *Circulation* 101: 886-892, 2000.
11. **Hagbarth KE, Vallbo AB.** Pulse and respiratory grouping of sympathetic impulses in human muscle-nerves. *Acta Physiol Scand* 74: 96-108. 1968.
12. **Hamner JW, Taylor JA.** Automated quantification of sympathetic beat-by-beat activity, independent of signal quality. *J Appl Physiol* 91: 1199-1206, 2001.
13. **Kamiya A, Hayano J, Kawada T, Michikami D, Yamamoto K, Ariumi H, Shimizu S, Uemura K, Miyamoto T, Aiba T, Sunagawa K, Sugimachi M.** Low-frequency oscillation of sympathetic nerve activity decreases during development of tilt-induced syncope preceding sympathetic withdrawal and bradycardia. *Am J Physiol* 289: H1758-H1769, 2005.
14. **Lambert E, Eikelis N, Esler M, Dawood T, Schlaich M, Bayles R, Socratous F, Agrotis A, Jennings G, Lambert G, Vaddadi G.** Altered sympathetic nervous reactivity and norepinephrine transporter expression in patients with postural tachycardia syndrome. *Circ Arrhythmia Electrophysiol* 1: 103-109. 2008.
15. **Malliani A, Pagani M, Lombardi F, Cerutti S.** Cardiovascular neural regulation explored in the frequency domain. *Circulation* 84: 482-492, 1991.

16. **Marchi A, Colombo R, Guzzetti S, Bari V, Bassani T, Raimondi F, Porta A.** Characterization of the cardiovascular control during modified head-up tilt test in healthy adult humans. *Auton Neurosci: Basic Clin* 179: 166-169, 2013.

17. **Montano N, Gnecchi-Ruscone T, Porta A, Lombardi F, Pagani M, Malliani A.** Power spectrum analysis of heart rate variability to assess the changes in sympathovagal balance during graded orthostatic tilt. *Circulation* 90: 1826-1831, 1994.

18. **Nakata A, Takata S, Yuasa T, Shimakura A, Maruyama M, Nagai H, Sakagami S, Kobayashi K.** Spectral analysis of heart rate, arterial pressure, and muscle sympathetic nerve activity in normal humans. *Am J Physiol* 274: H1211-H1217, 1998.

19. **O'Leary DD, Shoemaker JK, Edwards MR, Hughson RL.** Spontaneous beat-by-beat fluctuations of total peripheral and cerebrovascular resistance in response to tilt. *Am J Physiol* 287: R670-R679, 2004.

20. **Pagani M, Lombardi F, Guzzetti S, Rimoldi O, Furlan R, Pizzinelli P, Sandrone G, Malfatto G, Dell'Orto S, Piccaluga E, Turiel M, Baselli G, Cerutti S, Malliani A.** Power spectral analysis of heart rate and arterial pressure variabilities as a marker of sympatho-vagal interaction in man and conscious dog. *Circ Res* 59: 178-193, 1986.

21. **Pagani M, Montano N, Porta A, Malliani A, Abboud FM, Birkett C, Somers VK.** Relationship between spectral components of cardiovascular variabilities and direct measures of muscle sympathetic nerve activity in humans. *Circulation* 95: 1441-1448, 1997.

22. **Pomeranz B, Macaulay RJB, Caudill MA, Kutz I, Adam D, Gordon D, Kilborn KM, Barger AC, Shannon DC, Cohen RJ, Benson H.** Assessment of autonomic function in humans by heart-rate spectral-analysis, *Am J Physiol*, 248: H151-H153, 1985.

23. **Porta A, Tobaldini E, Guzzetti S, Furlan R, Montano N, Gnecchi-Ruscone T.** Assessment of cardiac autonomic modulation during graded head-up tilt by symbolic analysis of heart rate variability. *Am J Physiol* 293: H702-H708, 2007.

24. **Porta A, Catai AM, Takahashi ACM, Magagnin V, Bassani T, Tobaldini E, van de Borne P, Montano N.** Causal relationships between heart period and systolic arterial pressure during graded head-up tilt. *Am J Physiol* 300: R378-R386, 2011.

25. **Porta A, Bassani T, Bari V, Tobaldini E, Takahashi AC, Catai AM, Montano N.** Model-based assessment of baroreflex and cardiopulmonary couplings during graded head-up tilt. *Comput Biol Med* 42: 298-305, 2012.

26. **Ryan KL, Rickards CA, Hinojosa-Laborde C, Cooke WH, Convertino VA.** Arterial pressure oscillations are not associated with muscle sympathetic nerve activity in individuals exposed to central hypovolaemia. *J Physiol* 589: 5311-5322, 2011.

27. **Saul JP, Rea RF, Eckberg DL, Berger RD, Cohen RJ.** Heart rate and muscle sympathetic nerve variability during reflex changes of autonomic activity. *Am J Physiol* 258: H713-H721, 1990.

28. **Sundlof G, Wallin BG.** The variability of muscle nerve sympathetic activity in resting recumbent man. *J Physiol* 272: 383-397, 1977.

29. **Sundlof G, Wallin BG.** Human muscle nerve sympathetic activity at rest. Relationship to blood pressure and age. *J Physiol* 274: 621-637, 1978.

30. **Task Force of the European Society of Cardiology and the North American Society of Pacing and Electrophysiology.** Heart rate variability - Standards of measurement, physiological interpretation and clinical use. *Circulation* 93: 1043-1065, 1996.

587 31. **Taylor JA, Williams TD, Seals DR, Davy KP.** Low-frequency arterial pressure fluctuations do
588 not reflect sympathetic outflow: gender and age differences. *Am J Physiol* 274: H1194-H201,
589 1998.

590 32. **Wallin BG, Burke D, Gandevia S.** Coupling between variations in strength and baroreflex
591 latency of sympathetic discharges in human muscle nerves. *J Physiol* 474: 331-338, 1994.

592

Figure captions

Fig.1 Example of ECG, invasive AP, integrated MSNA, step-wise count MSNA and its low-pass filtered version during T60. The line plots show ECG (a, gain factor = 1000), invasive AP (b), integrated MSNA (c, gain factor = 1000), step-wise count MSNA derived from the integrated MSNA by counting the number of bursts occurring in a moving window of ΔT=5 s (d) and its low-pass filtered version obtained using a finite impulse response filter with a cut-off of 0.5 Hz (e). A slow rhythm with a period of about 12 s is visible in (d) and (e). The respiratory cycle in this example is about 4 s. Signals were recorded in the same subject during T60.

Fig.2 Examples of ucMSNA (a,b) and cMSNA (e,f) variability computed over the same subject during T0 (a,e) and during T60 (b,f). The corresponding autoregressive power spectral density (PSD) is plotted below the series (c,d,g,h).

Fig.3 Linear regression analysis of the LF_{cMSNA} and $LFnu_{ucMSNA}$ indexes on tilt table angles during graded orthostatic challenge. Individual values (open circles) of LF_{cMSNA} (a) and $LFnu_{ucMSNA}$ (b) indexes are shown as a function of the tilt table inclination (i.e. T0, T20, T30, T40, T60). Linear regression analysis is carried out and, if the slope of the regression line is significantly larger than 0 with $p<0.05$, the linear regression (solid line) and its 95 percent confidence interval (dotted lines) are plotted as well.

Fig.4 Linear regression analysis of the LF_{SAP}, LF_{DAP}, $LFnu_{HP}$ and HF_{HP} indexes on tilt table angles during graded orthostatic challenge. Individual values (open circles) of LF_{SAP} (a), LF_{DAP} (b), $LFnu_{HP}$ (c) and HF_{HP} (d) indexes are shown as a function of the tilt table inclination (i.e. T0, T20, T30, T40, T60). Linear regression analysis is carried out and, if the slope of the regression line is significantly larger than 0 with $p<0.05$, the linear regression (solid line) and its 95 percent confidence interval (dotted lines) are plotted as well.

Fig.5 Linear regression analysis of the LF_{SAP}, LF_{DAP}, $LFnu_{HP}$ and HF_{HP} indexes on the $LFnu_{ucMSNA}$ power during graded orthostatic challenge. Individual values (open circles) of LF_{SAP} (a), LF_{DAP} (b), $LFnu_{HP}$ (c) and HF_{HP} (d) indexes on the $LFnu_{ucMSNA}$ power after pooling all subjects together regardless of the experimental condition. Linear regression analysis is carried out and, if the slope of the regression line is significantly larger than 0 with $p<0.05$, the linear regression (solid line) and its 95 percent confidence interval (dotted lines) are plotted as well.

Fig.6 Linear regression analysis of the LF_{SAP}, LF_{DAP}, $LFnu_{HP}$ and HF_{HP} indexes on the LF_{cMSNA} power during graded orthostatic challenge. Individual values (open circles) of LF_{SAP} (a), LF_{DAP} (b), $LFnu_{HP}$ (c) and HF_{HP} (d) indexes on the LF_{cMSNA} power after pooling all subjects together regardless of the experimental condition. Linear regression analysis is carried out

627 and, if the slope of the regression line is significantly larger than 0 with $p<0.05$, the linear
628 regression (solid line) and its 95 percent confidence interval (dotted lines) are plotted as well.
629

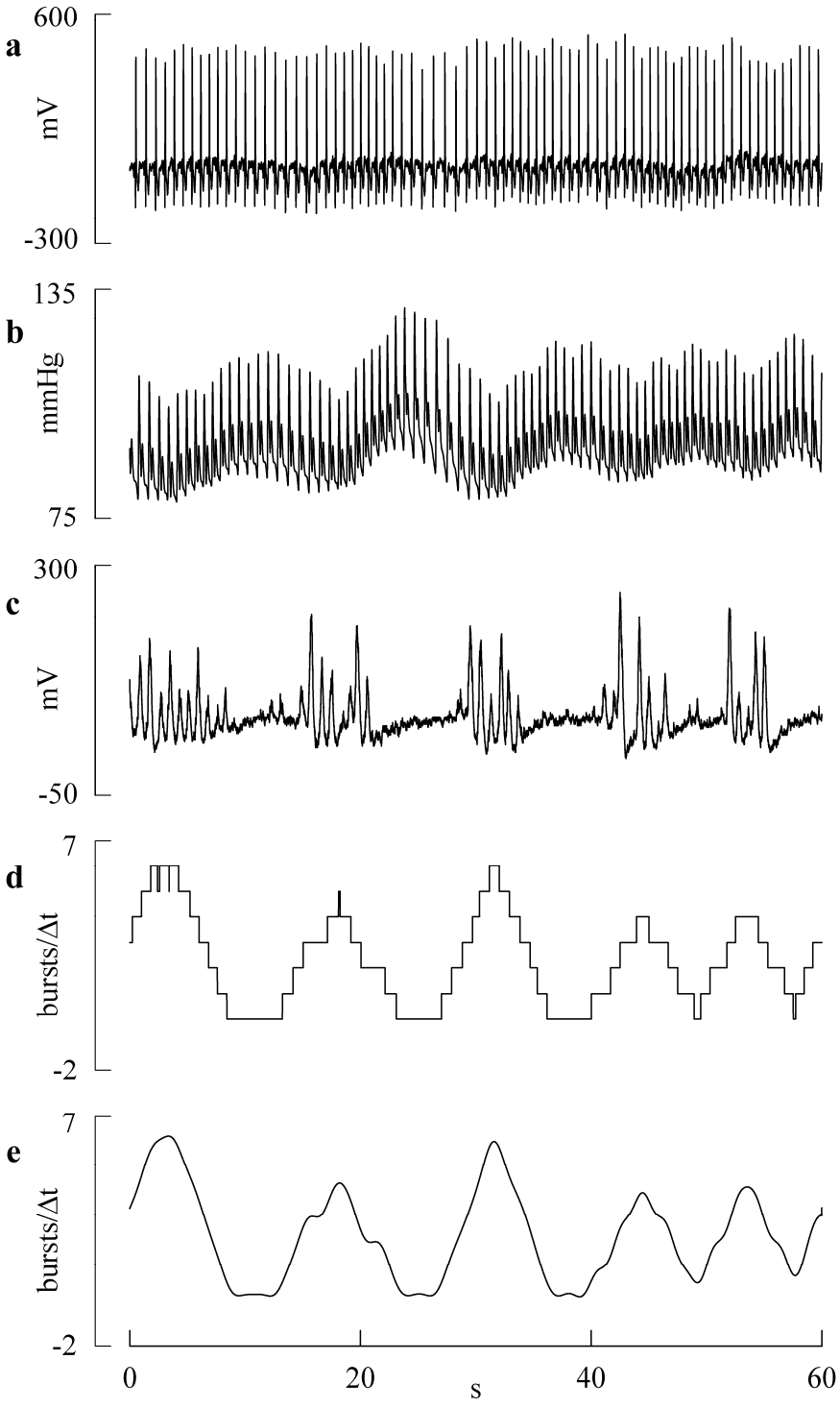
a
600
mV
-300
b
135
mmHg
75
c
300
mV
-50
d
7
bursts/Δt
-2
e
7
bursts/Δt
-2
0
20
40
60
s

Fig.1

634

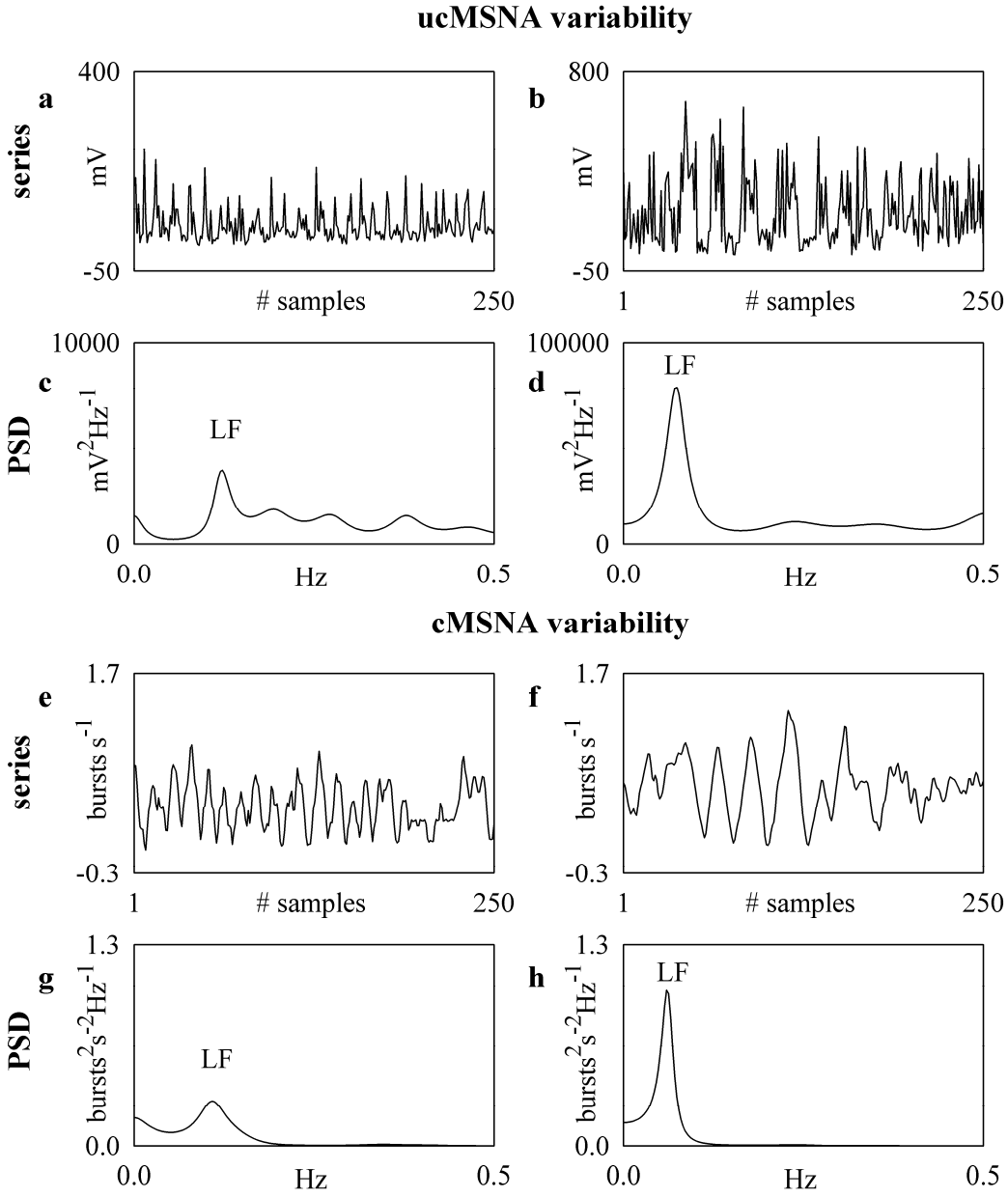

635

636 Fig.2

637

638

639

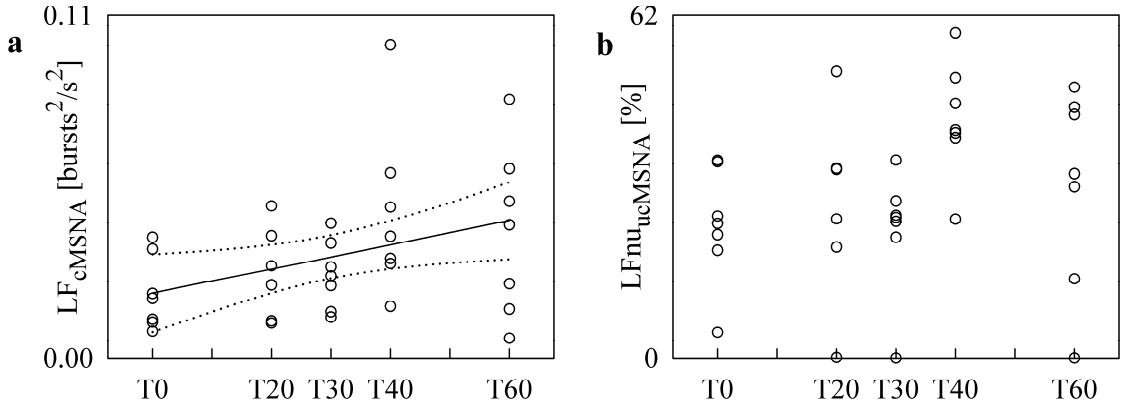

640

641 Fig.3

642

643

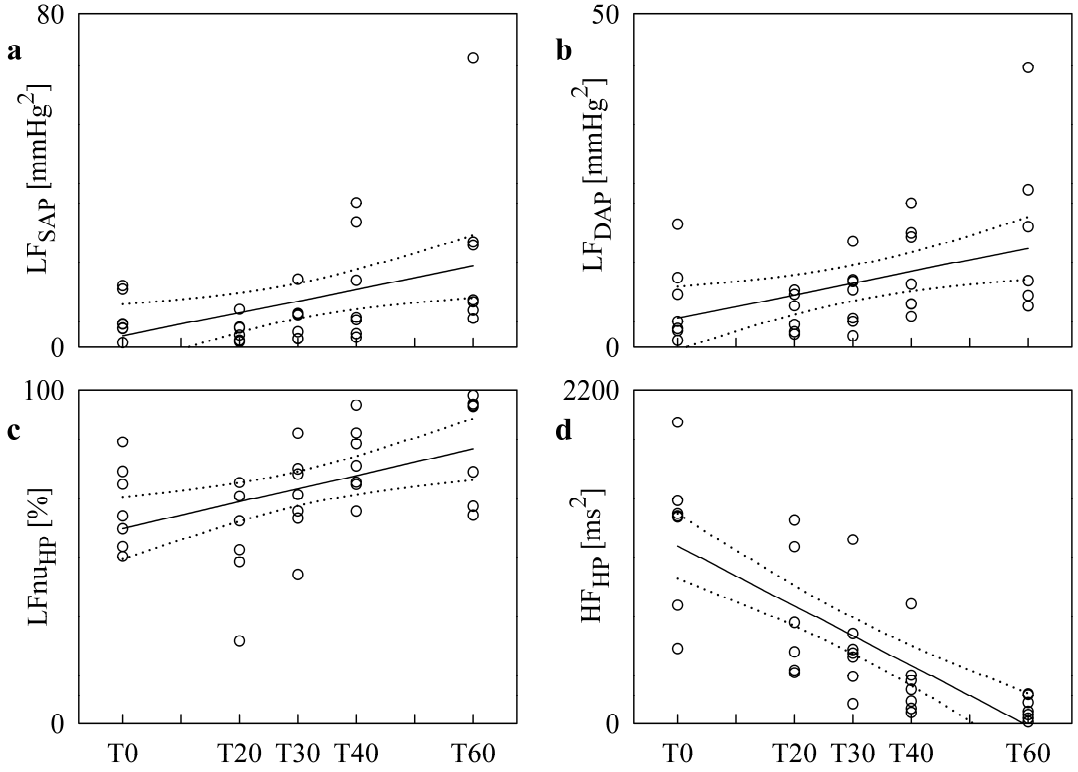

644

645

646 Fig.4

647

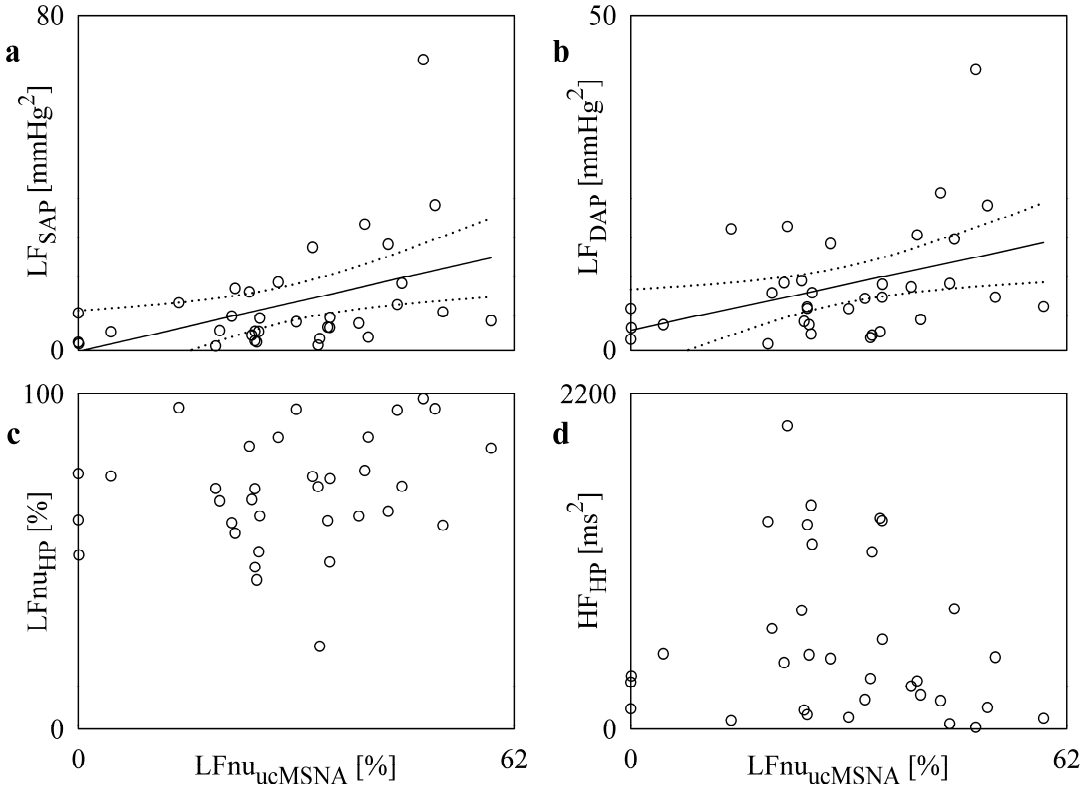
a
b
c
d
80
0
50
0
100
0
2200
0
62
62
LF_SAP [mmHg^2]
LF_DAP [mmHg^2]
LFnu_HP [%]
HF_HP [ms^2]
LFnu_ucMSNA [%]
LFnu_ucMSNA [%]

Fig.5

653

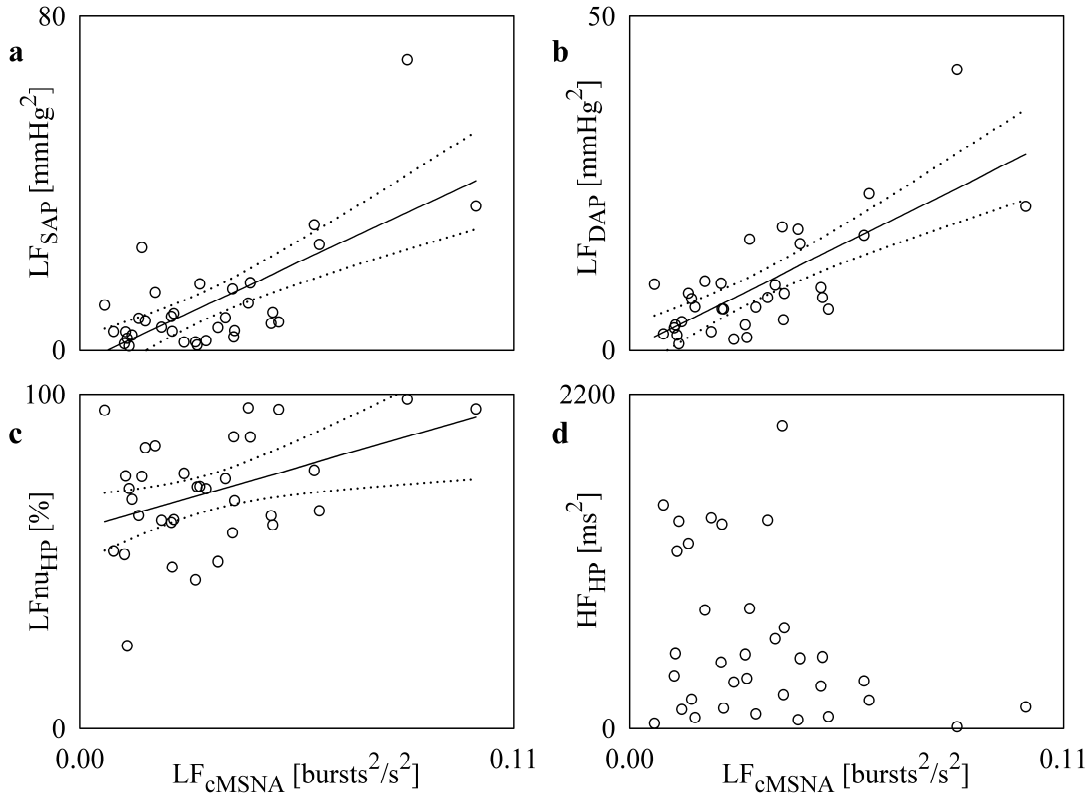

654

655

656 Fig.6

657

658

659 **Table 1.** Time domain parameters and NA data.

Index	T0	T20	T30	T40	T60
μ_{HP} [ms]	1003 ± 152	945 ± 145*	901 ± 134*	807 ± 122*	688 ± 120*
σ^2_{HP} [ms^2]	5239 ± 1071	2824 ± 1002*	4541 ± 2187	3266 ± 1803*	2498 ± 939*
μ_{SAP} [mmHg]	124.2 ± 16.2	122.7 ± 17.1	125.0 ± 17.1	122.3 ± 14.4	122.3 ± 16.7
σ^2_{SAP} [mmHg^2]	11.2 ± 8.8	9.4 ± 6.2	13.4 ± 8.4	22.2 ± 16.5	35.5 ± 22.2*
μ_{DAP} [mmHg]	68.8 ± 9.4	68.8 ± 10.9	69.4 ± 12.4	74.0 ± 11.1	75.5 ± 14.8*
σ^2_{DAP} [mmHg^2]	11.3 ± 8.5	9.3 ± 4.1	12.1 ± 6.1	15.5 ± 7.9	23.4 ± 10.9*
bf_{MSNA} [bursts/min]	19.0 ± 6.0	22.0 ± 5.9	26.1 ± 5.4*	29.6 ± 4.9*	26.3 ± 9.1*
bi_{MSNA} [bursts/100 beats]	31.1 ± 9.6	33.5 ± 6.4	38.3 ± 5.5	39.0 ± 3.3	29.3 ± 8.9
NA concentration [pg/ml]	129.7 ± 53.1	153.7 ± 76.1	214.3 ± 85.2	251.6 ± 116.2*	343.2 ± 252.1*
NA spillover [ng/min]	335.0 ± 165.3	329.0 ± 129.7	437.8 ± 132.2	497.7 ± 241.0	529.0 ± 529.4

660 μ_{HP} = HP mean; σ^2_{HP} = HP variance; μ_{SAP} = SAP mean; σ^2_{SAP} = SAP variance; μ_{DAP} = DAP mean; σ^2_{DAP} =
661 DAP variance; bf_{MSNA} = MSNA bursts frequency; bi_{MSNA} = MSNA bursts incidence; NA = plasma
662 noradrenaline; T0, T20, T30, T40, and T60 = head-up tilt at 0°, 20°, 30°, 40°, and 60°. Values are expressed
663 as mean ± standard deviation. The symbol * indicates $p < 0.05$ vs. T0.

664

665

666

667 **Table 2.** Frequency domain parameters.

Index	T0	T20	T30	T40	T60
$LFnu_{HP}$ [%]	65.1 ± 12.6	54.4 ± 17.2	68.0 ± 13.5	78.8 ± 10.8*	84.0 ± 15.8*
HF_{HP} [ms^2]	1264 ± 489	719 ± 434*	517 ± 342*	273 ± 245*	99 ± 73*
LF_{HP}/HF_{HP}	2.36 ± 1.57	1.49 ± 0.89	2.96 ± 1.88	7.52 ± 8.30	36.10 ± 59.10*
LF_{SAP} [$mmHg^2$]	7.08 ± 5.19	4.00 ± 2.88	6.75 ± 4.98	14.22 ± 13.19	22.44 ± 22.02*
LF_{DAP} [$mmHg^2$]	6.67 ± 6.17	5.03 ± 2.91	7.73 ± 4.86	11.75 ± 6.60	16.22 ± 13.10*
LF_{cMSNA} [$bursts^2/s^2$]	0.021 ± 0.012	0.027 ± 0.015	0.027 ± 0.011	0.047 ± 0.027*	0.040 ± 0.027
$LFnu_{ucMSNA}$ [%]	23.9 ± 10.6	27.6 ± 17.3	23.1 ± 11.1	43.2 ± 10.4	31.0 ± 18.0

668 nu= normalized units; $LFnu_{HP}$ = low frequency power of HP series expressed in nu; HF_{HP} = high frequency
669 power of HP series; LF_{HP}/HF_{HP} = the ratio of the LF to the HF powers computed over HP series; LF_{SAP} = low
670 frequency power of SAP series; LF_{DAP} = low frequency power of DAP series; LF_{cMSNA} = low frequency
671 power of the cMSNA series; $LFnu_{ucMSNA}$ = low frequency power of the ucMSNA series expressed in nu; T0,
672 T20, T30, T40, and T60 = head-up tilt at 0°, 20°, 30°, 40°, and 60°. Values are expressed as mean ± standard
673 deviation. The symbol * indicates $p < 0.05$ vs. T0.

674

675

676

677 **Table 3.** Results of the linear correlation analysis between NA data and frequency domain
678 parameters.

Index	NA concentration		NA spillover	
	r	*p*	*r*	*p*
$LFnu_{HP}$	0.163	$3.71 \cdot 10^{-1}$	-0.120	$5.38 \cdot 10^{-1}$
HF_{HP}	-0.369	$3.79 \cdot 10^{-2}$ *	-0.0301	$8.77 \cdot 10^{-1}$
LF_{HP}/HF_{HP}	0.229	$2.05 \cdot 10^{-1}$	-0.0739	$7.06 \cdot 10^{-1}$
LF_{SAP}	0.577	$5.84 \cdot 10^{-4}$ *	0.227	$2.43 \cdot 10^{-1}$
LF_{DAP}	0.579	$5.49 \cdot 10^{-4}$ *	0.210	$2.80 \cdot 10^{-1}$
LF_{cMSNA}	0.445	$1.09 \cdot 10^{-2}$ *	0.0996	$6.11 \cdot 10^{-1}$
$LFnu_{ucMSNA}$	0.423	$1.61 \cdot 10^{-2}$ *	0.182	$3.50 \cdot 10^{-1}$

679 nu= normalized unit; $LFnu_{HP}$ = low frequency power of HP series expressed in nu; HF_{HP} = high frequency
680 power of HP series; LF_{HP}/HF_{HP} = the ratio of the LF to the HF powers computed over HP series; LF_{SAP} = low
681 frequency power of SAP series; LF_{DAP} = low frequency power of DAP series; LF_{cMSNA} = low frequency
682 power of the cMSNA series; $LFnu_{ucMSNA}$ = low frequency power of the ucMSNA series expressed in nu; NA
683 = plasma noradrenaline; *r* = Pearson product-moment correlation coefficient; *p* = type I error probability.
684 The symbol * indicates a $p < 0.05$.

685

686

687

688

689 **Table 4.** Fraction of subjects exhibiting a squared correlation coefficient, r^2,
690 larger than 0.5 between SAP or DAP spectral markers and MSNA
691 variability indexes in the LF band during graded head-up tilt protocol.

Type of analysis	$r^2>0.5$
LF_{SAP} vs $LFnu_{ucMSNA}$	2/7
LF_{SAP} vs LF_{cMSNA}	5/7
LF_{DAP} vs $LFnu_{ucMSNA}$	1/7
LF_{DAP} vs LF_{cMSNA}	5/7

692 nu= normalized units; LF_{SAP} = low frequency power of SAP series; LF_{DAP} = low
693 frequency power of DAP series; LF_{cMSNA} = low frequency power of the cMSNA
694 series; $LFnu_{ucMSNA}$ = low frequency power of the ucMSNA series expressed in nu.

695

696

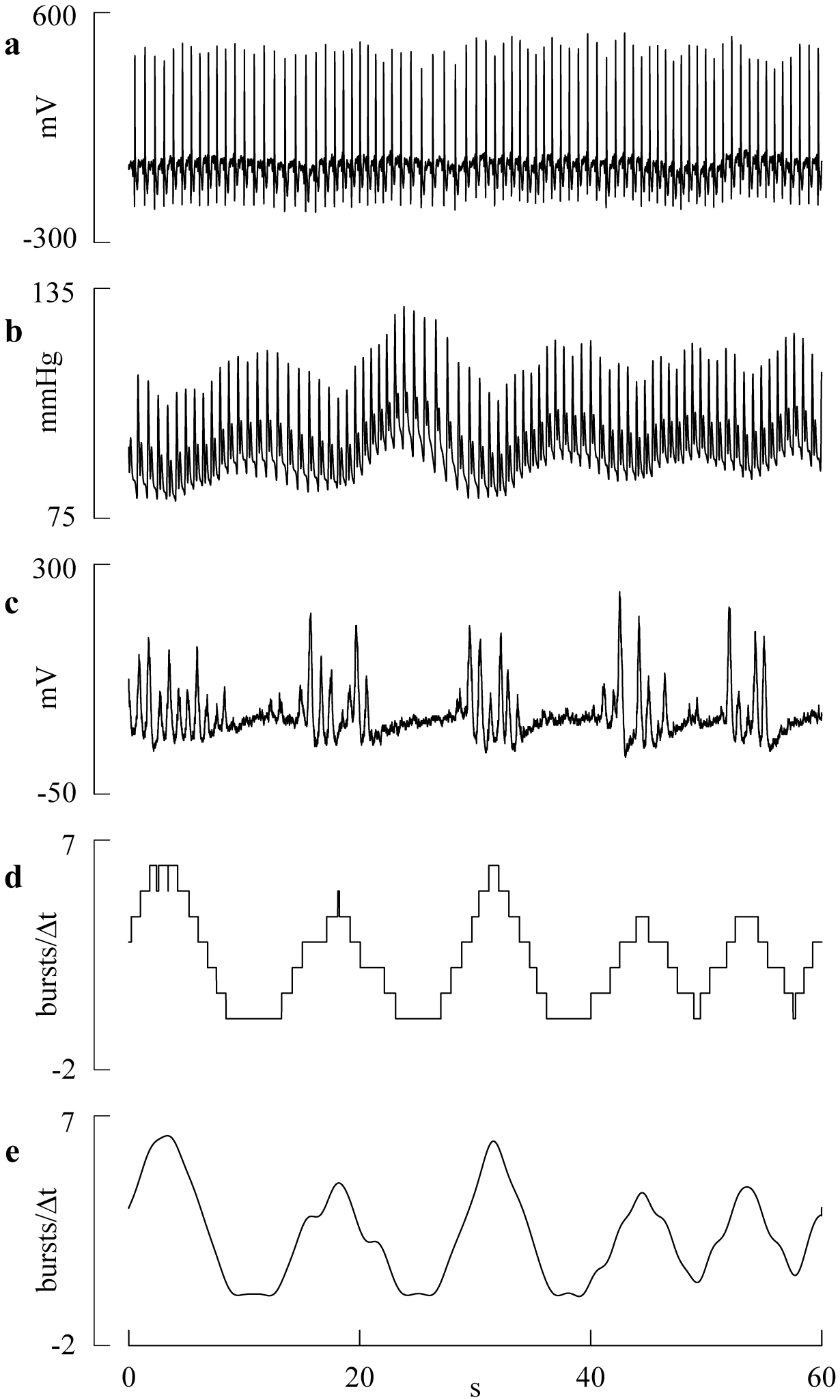
a
600
mV
-300
b
135
mmHg
75
c
300
mV
-50
d
7
bursts/Δt
-2
e
7
bursts/Δt
-2
0
20
40
60
s

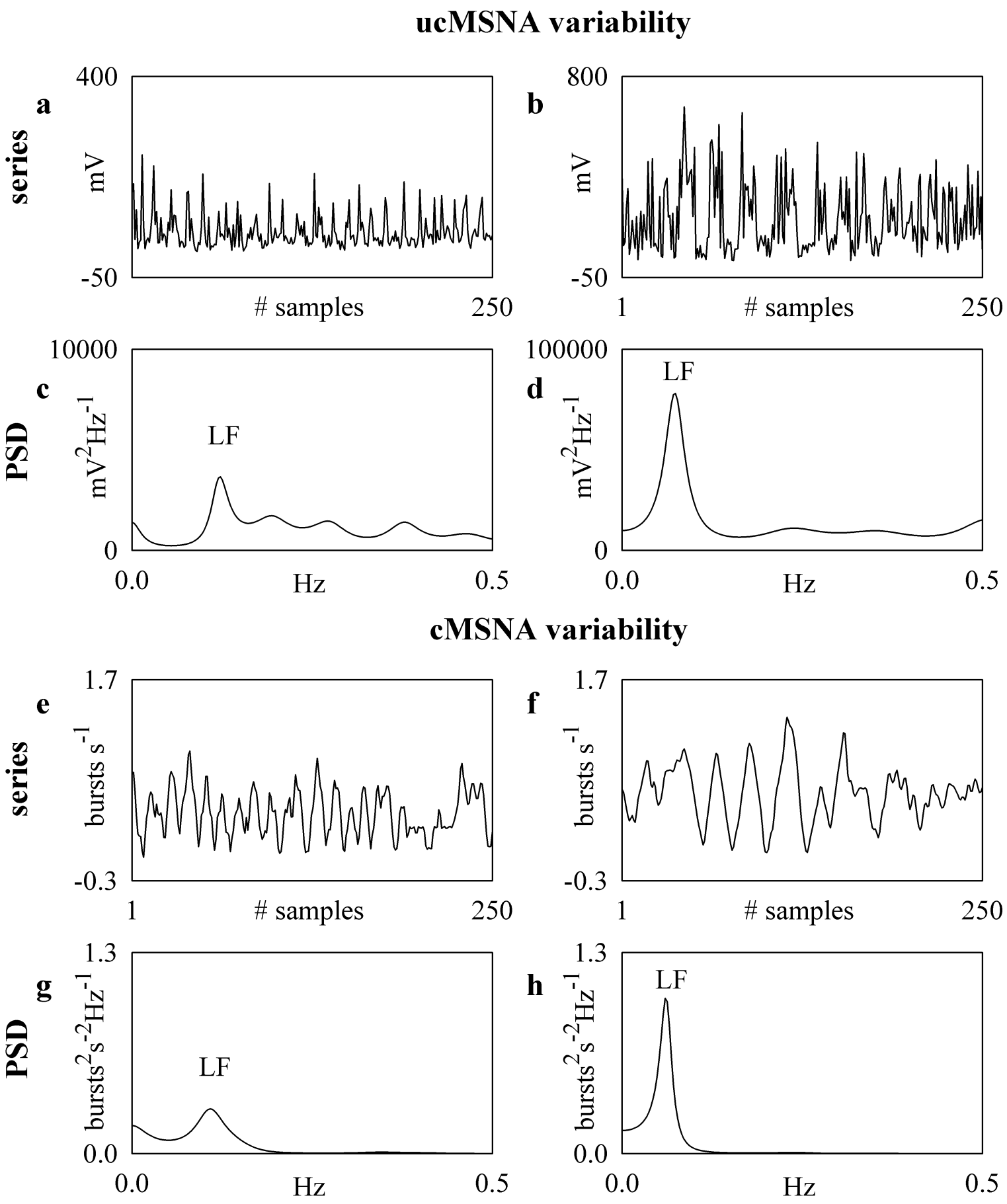
ucMSNA variability
a
b
series
400
-50
mV
samples
250
800
1
c
d
PSD
10000
0
mV²Hz⁻¹
LF
100000
0.0
Hz
0.5
cMSNA variability
e
f
1.7
-0.3
bursts s⁻¹
g
h
1.3
0.0
bursts²s⁻²Hz⁻¹

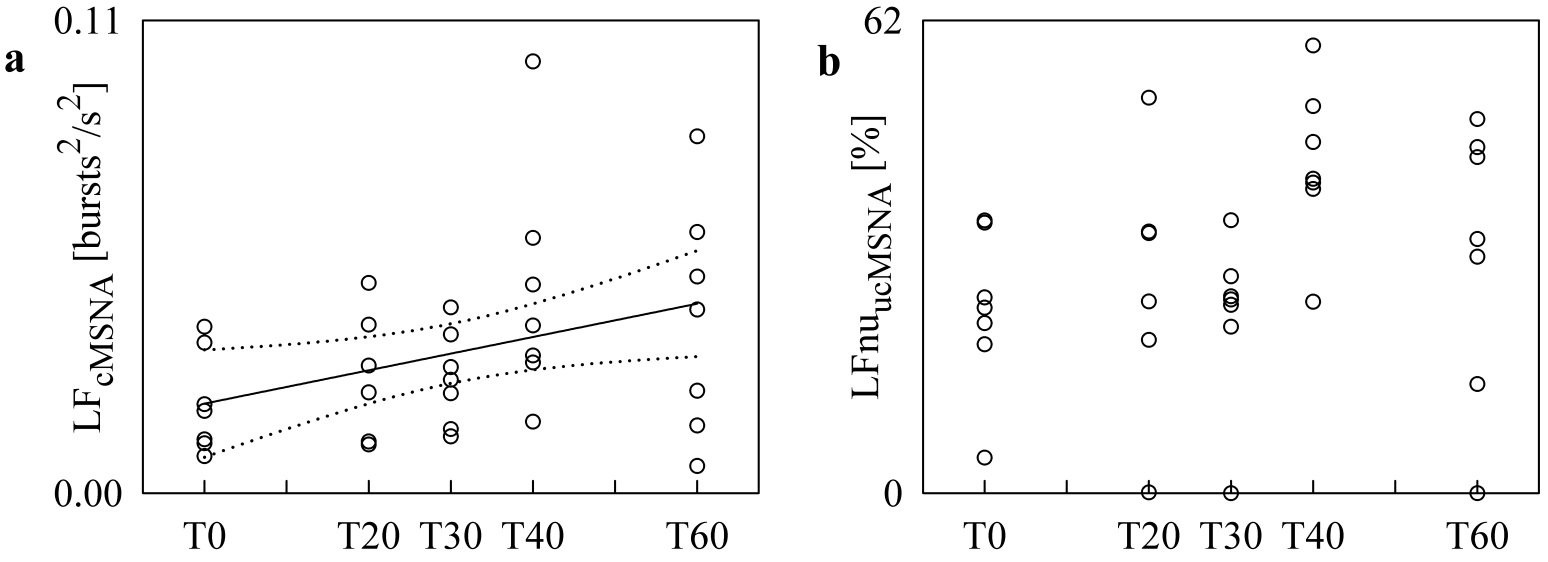
a
0.11
0.00
LF cMSNA [bursts²/s²]
T0
T20
T30
T40
T60
b
62
0
LFnu ucMSNA [%]
T0
T20
T30
T40
T60

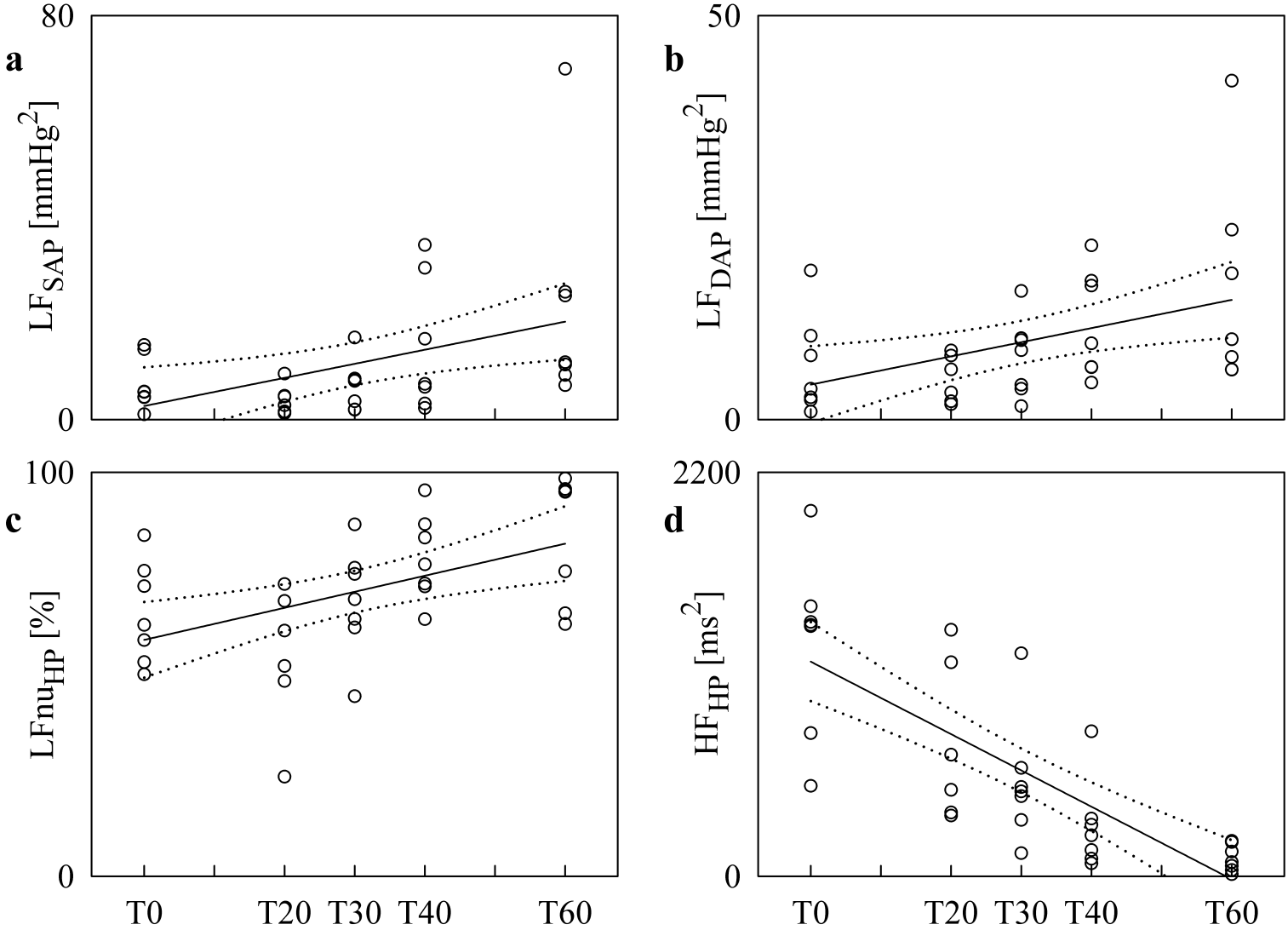
a
80
0
LF_{SAP} [$mmHg^2$]
b
50
0
LF_{DAP} [$mmHg^2$]
c
100
0
$LFnu_{HP}$ [%]
d
2200
0
HF_{HP} [ms^2]
T0
T20
T30
T40
T60

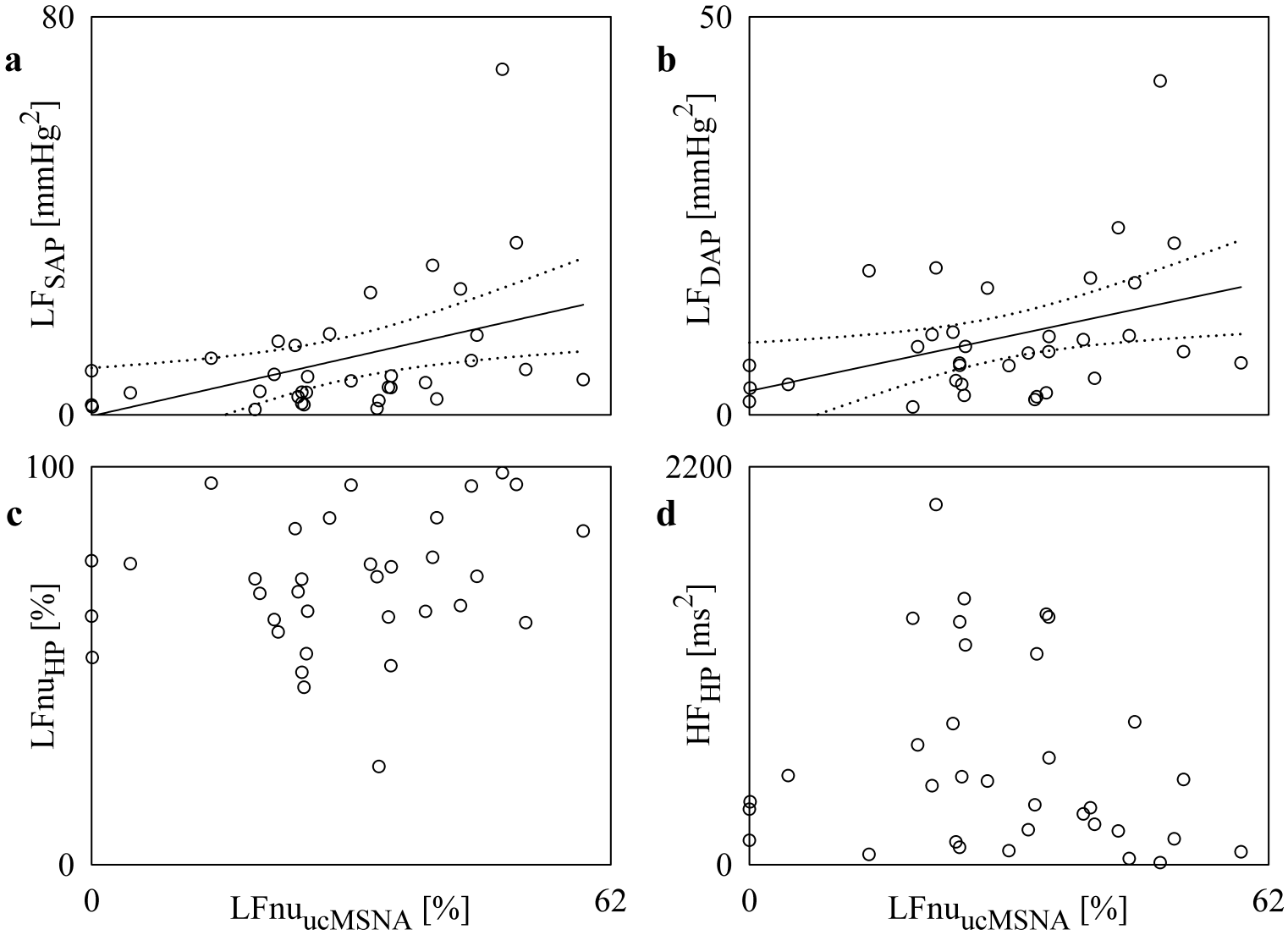
a
80
0
LF_{SAP} [$mmHg^2$]
b
50
0
LF_{DAP} [$mmHg^2$]
c
100
0
$LFnu_{HP}$ [%]
d
2200
0
HF_{HP} [ms^2]
0
$LFnu_{ucMSNA}$ [%]
62
0
$LFnu_{ucMSNA}$ [%]
62

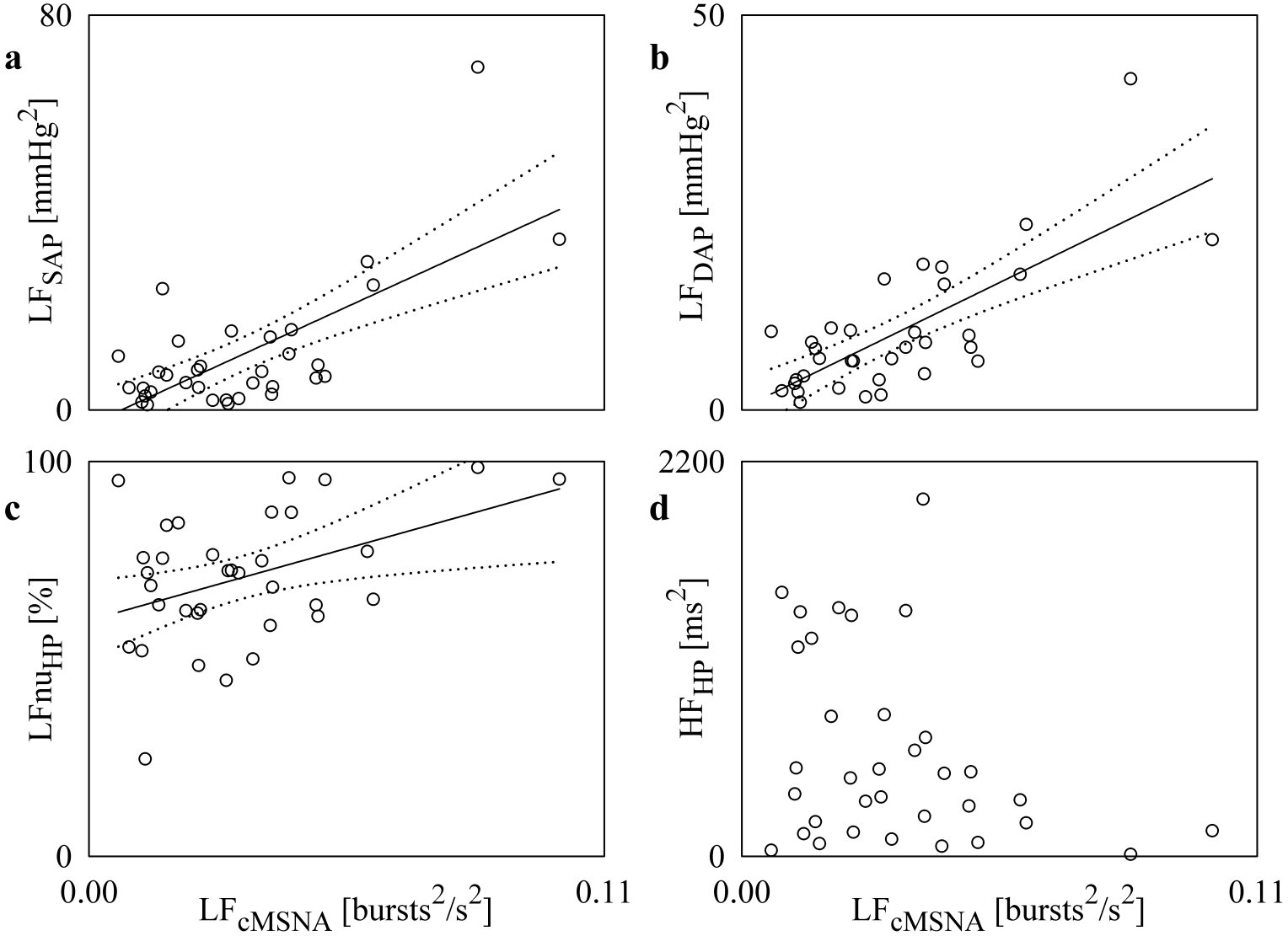
a
80
0
LF_{SAP} [$mmHg^2$]
b
50
0
LF_{DAP} [$mmHg^2$]
c
100
0
$LFnu_{HP}$ [%]
d
2200
0
HF_{HP} [ms^2]
0.00
0.11
LF_{cMSNA} [$bursts^2/s^2$]
0.00
0.11
LF_{cMSNA} [$bursts^2/s^2$]

Table 1. Time domain parameters and NA data.

Index	T0	T20	T30	T40	T60
μ_{HP} [ms]	1003 ± 152	945 ± 145*	901 ± 134*	807 ± 122*	688 ± 120*
σ^2_{HP} [ms^2]	5239 ± 1071	2824 ± 1002*	4541 ± 2187	3266 ± 1803*	2498 ± 939*
μ_{SAP} [mmHg]	124.2 ± 16.2	122.7 ± 17.1	125.0 ± 17.1	122.3 ± 14.4	122.3 ± 16.7
σ^2_{SAP} [mmHg^2]	11.2 ± 8.8	9.4 ± 6.2	13.4 ± 8.4	22.2 ± 16.5	35.5 ± 22.2*
μ_{DAP} [mmHg]	68.8 ± 9.4	68.8 ± 10.9	69.4 ± 12.4	74.0 ± 11.1	75.5 ± 14.8*
σ^2_{DAP} [mmHg^2]	11.3 ± 8.5	9.3 ± 4.1	12.1 ± 6.1	15.5 ± 7.9	23.4 ± 10.9*
bf_{MSNA} [bursts/min]	19.0 ± 6.0	22.0 ± 5.9	26.1 ± 5.4*	29.6 ± 4.9*	26.3 ± 9.1*
bi_{MSNA} [bursts/100 beats]	31.1 ± 9.6	33.5 ± 6.4	38.3 ± 5.5	39.0 ± 3.3	29.3 ± 8.9
NA concentration [pg/ml]	129.7 ± 53.1	153.7 ± 76.1	214.3 ± 85.2	251.6 ± 116.2*	343.2 ± 252.1*
NA spillover [ng/min]	335.0 ± 165.3	329.0 ± 129.7	437.8 ± 132.2	497.7 ± 241.0	529.0 ± 529.4

μ_{HP} = HP mean; σ^2_{HP} = HP variance; μ_{SAP} = SAP mean; σ^2_{SAP} = SAP variance; μ_{DAP} = DAP mean; σ^2_{DAP} = DAP variance; bf_{MSNA} = MSNA bursts frequency; bi_{MSNA} = MSNA bursts incidence; NA = plasma noradrenaline; T0, T20, T30, T40, and T60 = head-up tilt at 0°, 20°, 30°, 40°, and 60°. Values are expressed as mean ± standard deviation. The symbol * indicates $p < 0.05$ vs. T0.

Table 2. Frequency domain parameters.

Index	T0	T20	T30	T40	T60
$LFnu_{HP}$ [%]	65.1 ± 12.6	54.4 ± 17.2	68.0 ± 13.5	78.8 ± 10.8*	84.0 ± 15.8*
HF_{HP} [ms^2]	1264 ± 489	719 ± 434*	517 ± 342*	273 ± 245*	99 ± 73*
LF_{HP}/HF_{HP}	2.36 ± 1.57	1.49 ± 0.89	2.96 ± 1.88	7.52 ± 8.30	36.10 ± 59.10*
LF_{SAP} [$mmHg^2$]	7.08 ± 5.19	4.00 ± 2.88	6.75 ± 4.98	14.22 ± 13.19	22.44 ± 22.02*
LF_{DAP} [$mmHg^2$]	6.67 ± 6.17	5.03 ± 2.91	7.73 ± 4.86	11.75 ± 6.60	16.22 ± 13.10*
LF_{cMSNA} [$bursts^2/s^2$]	0.021 ± 0.012	0.027 ± 0.015	0.027 ± 0.011	0.047 ± 0.027*	0.040 ± 0.027
$LFnu_{ucMSNA}$ [%]	23.9 ± 10.6	27.6 ± 17.3	23.1 ± 11.1	43.2 ± 10.4	31.0 ± 18.0

nu= normalized units; $LFnu_{HP}$ = low frequency power of HP series expressed in nu; HF_{HP} = high frequency power of HP series; LF_{HP}/HF_{HP} = the ratio of the LF to the HF powers computed over HP series; LF_{SAP} = low frequency power of SAP series; LF_{DAP} = low frequency power of DAP series; LF_{cMSNA} = low frequency power of the cMSNA series; $LFnu_{ucMSNA}$ = low frequency power of the ucMSNA series expressed in nu; T0, T20, T30, T40, and T60 = head-up tilt at 0°, 20°, 30°, 40°, and 60°. Values are expressed as mean ± standard deviation. The symbol * indicates $p < 0.05$ vs. T0.

Table 3. Results of the linear correlation analysis between NA data and frequency domain parameters.

Index	NA concentration		NA spillover	
	r	*p*	*r*	*p*
$LFnu_{HP}$	0.163	$3.71 \cdot 10^{-1}$	-0.120	$5.38 \cdot 10^{-1}$
HF_{HP}	-0.369	$3.79 \cdot 10^{-2}$ *	-0.0301	$8.77 \cdot 10^{-1}$
LF_{HP}/HF_{HP}	0.229	$2.05 \cdot 10^{-1}$	-0.0739	$7.06 \cdot 10^{-1}$
LF_{SAP}	0.577	$5.84 \cdot 10^{-4}$ *	0.227	$2.43 \cdot 10^{-1}$
LF_{DAP}	0.579	$5.49 \cdot 10^{-4}$ *	0.210	$2.80 \cdot 10^{-1}$
LF_{cMSNA}	0.445	$1.09 \cdot 10^{-2}$ *	0.0996	$6.11 \cdot 10^{-1}$
$LFnu_{ucMSNA}$	0.423	$1.61 \cdot 10^{-2}$ *	0.182	$3.50 \cdot 10^{-1}$

nu= normalized unit; $LFnu_{HP}$ = low frequency power of HP series expressed in nu; HF_{HP} = high frequency power of HP series; LF_{HP}/HF_{HP} = the ratio of the LF to the HF powers computed over HP series; LF_{SAP} = low frequency power of SAP series; LF_{DAP} = low frequency power of DAP series; LF_{cMSNA} = low frequency power of the cMSNA series; $LFnu_{ucMSNA}$ = low frequency power of the ucMSNA series expressed in nu; NA = plasma noradrenaline; *r* = Pearson product-moment correlation coefficient; *p* = type I error probability. The symbol * indicates a $p < 0.05$.

Table 4. Fraction of subjects exhibiting a squared correlation coefficient, r^2, larger than 0.5 between SAP or DAP spectral markers and MSNA variability indexes in the LF band during graded head-up tilt protocol.

Type of analysis	$r^2>0.5$
LF_{SAP} vs $LFnu_{ucMSNA}$	2/7
LF_{SAP} vs LF_{cMSNA}	5/7
LF_{DAP} vs $LFnu_{ucMSNA}$	1/7
LF_{DAP} vs LF_{cMSNA}	5/7

nu= normalized units; LF_{SAP} = low frequency power of SAP series; LF_{DAP} = low frequency power of DAP series; LF_{cMSNA} = low frequency power of the cMSNA series; $LFnu_{ucMSNA}$ = low frequency power of the ucMSNA series expressed in nu.